DEEP-DRAWING PROCESS ANALYSIS OF ELLIPTIC CUPS BY RIGID-PLASTIC FEM①

Chang, Zhihua Ma, Yanwei② Huang, Shangyu Jiang, Kuihua
Department Mechanical Engineering No. 2, Wuhan Institute of Technology, Wuhan 430070

ABSTRACT

The deformation characteristics of elliptic cups were studied through simulating their deep-drawing deformation processes using rigid-plastic finite element method(FEM), and the influence was analysed of ellipticity(a/b) on strain distribution in deformation zone and formation limit. The results showed that because deep-drawing workpieces and their developed views are non-rotary, their deep-drawing deformation is non-uniform, i. e. along the outer fringe of the deformation zone, where the larger the curvature, the larger the deformation degree, and the formation limit depends greatly on the ellipticity.

Key words: elliptic cups deep-drawing formation limit rigid-plastic finite element method

1 INTRODUCTION

Straight wall workpieces with elliptic openings, i. e. elliptic cups, are typical non-rotary workpieces, and have been used as intermediate blanks in deep-drawing rectangular boxes with large depths[1]. The knowledge about the stamping deformation characteristics of the elliptic cups is essential for analyzing the stamping forming processes of workpieces with more complicated shapes. In recent years, attention has been paid to the inhomogenity of metal flow in the deformation zone of the elliptic cups deep-drawing[2,3]. CAD programs for selecting reasonable blanks of standard elliptic deep-drawing workpieces have also been developed using the slip line field theory and with the help of computer-aided design[4]. However, little work has been done on the distribution characteristics of metal flow in the deformation zone, the influence of the ellipticity a/b and the formation limit of primary drawing. Few papers have been reported on the study of simulating the forming processes of sheet metals by the rigid-plastic FEM, and the published work mainly involves the problems in the deep-drawing processes of the elliptic cups and rectangular boxes[5,6]. Therefore, the existing theories are fairly insufficient for laying out stamping forming processes of the circular cups. This paper studied the deformation law of the elliptic cups deep-drawing processes by the rigid-plastic FEM, and was aimed at supplying some necessary information for probing the forming mechanisms of the workpieces of this kind, and laying out reasonable stamping processes, which is undoubtedly of great importance for practical production.

2 PRINCIPLE OF RIGID-PLASTIC FEM

Deformation of sheet metals deep-drawing mainly occurs in the flange area. When the strain along the sheet thickness is far smaller than the two principal strains on the sheet plane, the change of the sheet thickness in the deep-drawing process can be neglected and the deep-drawing deformation can be treated as a plane strain problem. Assuming that the metals satisfy rigid-plastic conditions, a functional can be established as follows using incompletely generalized variational principle:

① Manuscript received May 25, 1993, translated by Ou, Yinglong
② Works at Qinghua University

$$\varphi = \sqrt{2}K\int_V \sqrt{\{\dot{\varepsilon}\}^T\{\dot{\varepsilon}\}}\mathrm{d}V - \int_{S_p}\{p\}^T\{u\}\mathrm{d}S + \int_V \lambda\{\dot{\varepsilon}\}^T\{c\}\mathrm{d}V \quad (1)$$

where $\{\dot{\varepsilon}\}$ — column matrix of strain rates; $\{u\}$— columm matrix of velocities; $\{p\}$— column matrix of surface forees on stress boundary S_p; $\{c\}$—matrix symbols, in this paper, $\{c\}=[1, 1, 0]^T$; λ —Lagrange′ s multiplier; K —shear yield strength.

For a rigid-plastic continuous body of volume V and with given stress boundary S_p and velocity boundary S_u, without consideration of its volumetric force, then among the velocity fields which satisfy strain rate relations and given velocity boundary conditions, those dynamic compatibility velocity fields which can make the above functional obatin stationary values are sure to be true velocity fields, and the value of λ is the average stress in the continuous body.

In order to approach the true solutions of the problem, divide the continuous body into M units with N nodes connected. The strain rate field in each unit is:

$$\{\dot{\varepsilon}\} = \{\dot{\varepsilon}_x, \dot{\varepsilon}_y, \dot{\gamma}_{xy}\}^T = \{\frac{\partial u}{\partial x}, \frac{\partial v}{\partial y}, \frac{\partial u}{\partial y} + \frac{\partial v}{\partial x}\} = [B]\{u\} \quad (2)$$

Assuming a displacement mode for each unit, there will be an assumed velocity field correspondingly whose functional $\varphi^{(m)}$ is:

$$\varphi^{(m)} = \sqrt{3}K\int_{V^{(m)}} \sqrt{2/3\{u\}^T[A]\{u\}}\mathrm{d}V - \{u\}^T\{F\} + \lambda^{(m)}\{u\}^T\{Q\} \quad (3)$$

where $[A] = [B]^T[B]$;

$$\{F\} = \int_{S_p^{(m)}}[N]^T\{p\}\mathrm{d}S;$$

$$\{Q\} = \int_{V^{(m)}}[B]^T\{c\}\mathrm{d}V;$$

$[N]$ —shape function of the unit.

$\{u\}$ and λ obtained from the variation equation of

$$\delta\varphi = \delta(\sum_{m=1}^{M}\varphi^{(m)}) = 0 \quad (4)$$

are true solutions.

3 DEFORMATION ANALYSIS OF DEEP-DRAWING PROCESS BY FEM

In the deformation analysis of the elliptic cup deep-drawing processes by the rigid-plastic FEM, the grids were automatically formed using the parameter variation method, and the flange area of the blank was divided into several 4-node units. According to Nadai′ s idea, the moving velocity of the blank should be paid attention to in consideration of the friction between the blank and the tool. When the moving velocity of the blank is smaller than a certain critical value, it can be believed that the frictional force is linearly dependent on it. Otherwise, the frictional force is a constant.

At the mouth of the female die, the metal flows along the round corner of it. It does not deform after it turns into the cup wall and its moving velocity equals that of the punch. Therefore, the increasing load can be realized through controlling the downward displacement of the drift. After each increment calculation, the displacement of each node and the deformation of each grid are known, and the flange contour of the workpiece can be obtained by connecting the boundary nodes successively.

Due to the inhomogeneity of deformation of the elliptic cup deep-drawing, the velocities of the metal particles on the flange area flowing into the female die will not be equivalent. After each increment calculation, some corrections on the boundary conditions are necessary, so as to ensure all along the inner boundary of the deformation zone coincide with the contour of the concave die mouth, and re-treat the grids on the flange area. Fig. 1 shows the change of the grids on the flange area in simulating different deep-drawing heights.

After the amount of data obtained from simulating analysis are dealt with by computer program, simple and clear results are presented in forms of graphs, curves and tables. Fig. 2 is the block diagram of the FEM analysis program.

4 RESULTS AND DISCUSSION

The FEM analysis program was run on an ALR 386/222 computer. The property parameters of the studied material are listed in Taole 1, and the hardening curve can be expressed by $\bar{\sigma} = K\bar{\varepsilon}^n$.

4.1 *Velocity Distribution Characteristics in Deformation Zone*

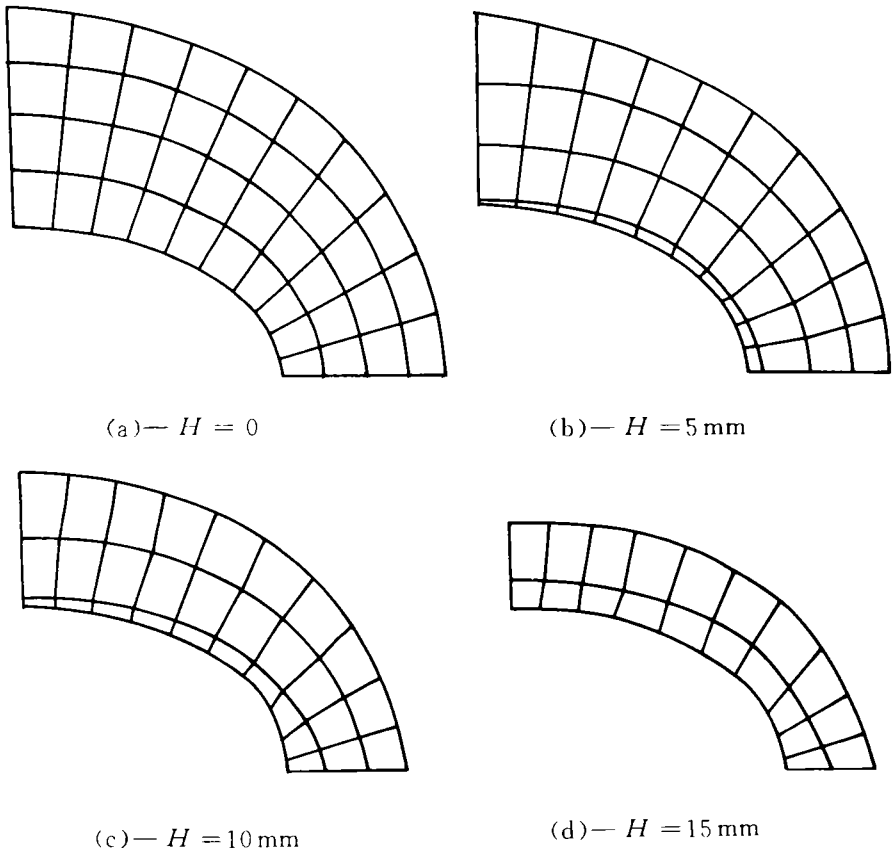

(a)— $H = 0$ (b)— $H = 5\,\text{mm}$

(c)— $H = 10\,\text{mm}$ (d)— $H = 15\,\text{mm}$

Fig. 1 Change patterns of grids on flange area

The velocity distribution pattern obtained by the FEM analysis is shown in Fig. 3. Along the outer fringe of the flange area, i. e. the outer fringe of the deformation zone, the moving velocities of the metal particles are not equivalent. The moving velocity at point A is smaller than that at point B, which makes the velocity gradient along the major axis (x-axis) larger than that along the minor axis (y-axis). This indicates that the larger the curvature is, the larger the radial lengthening deformation and the latitudinal compression deformation are. Fig. 3 presents the case of $a/b = 1.6$ and in this case $u_A/u_B = 0.31$. If the ratio of a/b increases, the curvature difference between point A and point B will increase and correspondingly the difference of moving velocities will also increase.

4.2 *Effective Stress and Strain Distribution*

The effective strain distribution of the elliptic cup with a punching depth of 5 mm and an axial ratio $a/b = 1.6$ is shown in Fig. 4(a). It is clear that in the elliptic cup deep-drawing, the strain distribution along the inner and outer fringe of the deformation zone is nonuniform and the deformation along the major axis (x-axis) is fairly violent.

Because where the curvature is larger, the deformation resistance is larger and the deformation resistance and deformation distributions are nonuniform, there occurs shear deformation in each unit. The existence of the shear deformation can help adjust the deformation in different units and reduce the difference of deformation degrees between the particles of larger curvature and those of smaller curvature.

The effective stress distribution of the metal on the fringe (the inner boundary of the deformation zone) calculated by the FEM is shown in Fig. 4(b). It is evident that the larger the curvature, the larger the effective stress, i. e. the radial

tensile stress σ_r is larger than those at other points. Therefore, the rupture of the elliptic cups deep-drawing also occurs there first.

5 APPLICATION OF FEM ANALYSIS

In the metal forming field, the FEM analysis

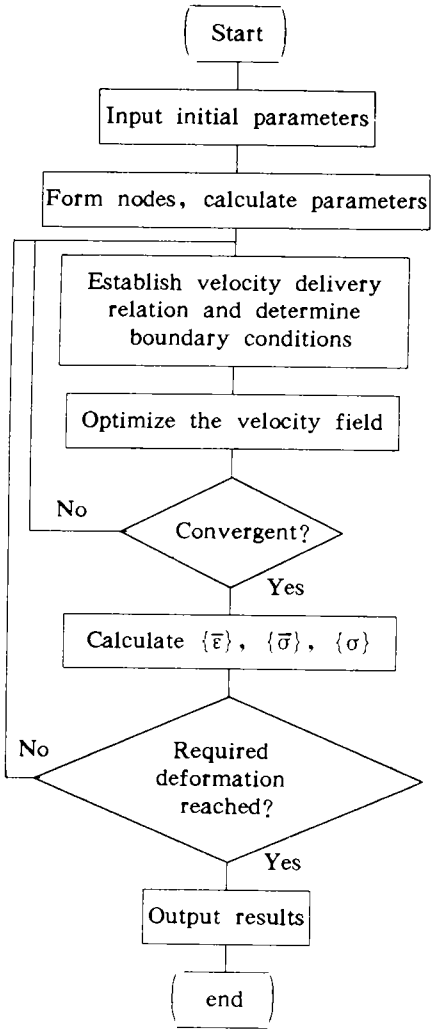

Fig. 2 Block diagram of FEM analysis program

Table 1 Property parameters of the studied material*

material	σ_s /MPa	K /MPa	n	r	t /mm
galvanized steel sheet	220.42	583	0.21	1.22	1

* : n —hardening index; r —coefficient of normal anisotropy; t —sheet thickness

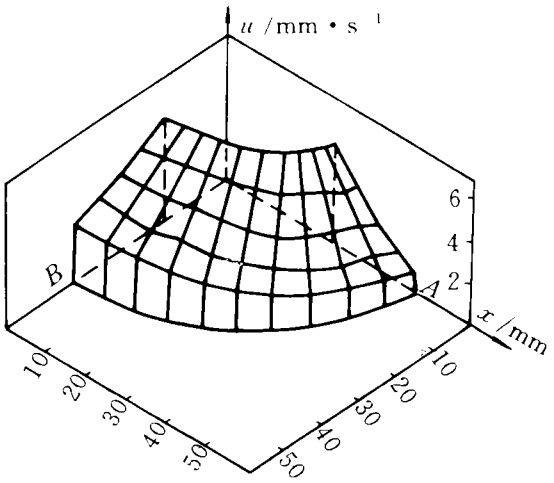

Fig. 3 Velocity distribution pattern in deformation zone

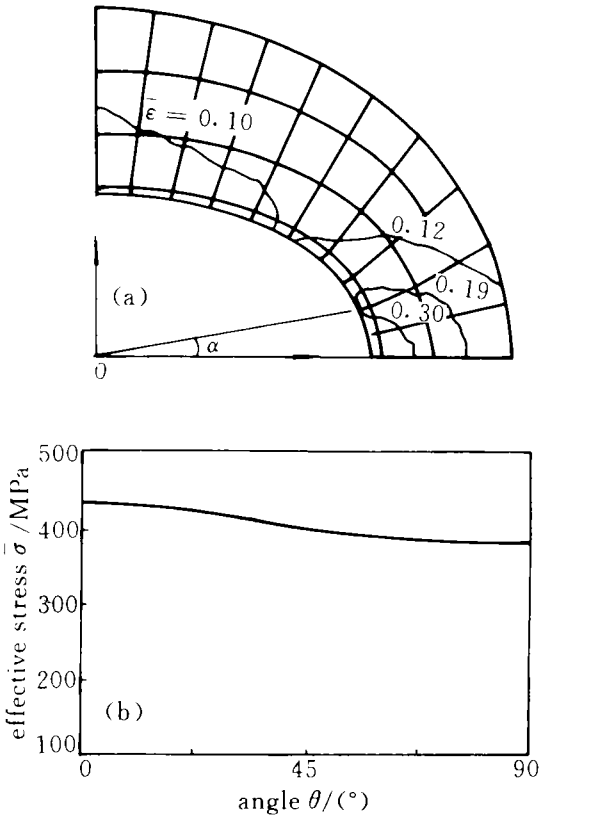

Fig. 1 Effective stress and strain distribution patterns

(a) effective strain distribution pattern;

(b) effective stress distribution pattern

technique can supply an effective means for probing various theoretical problems in the metal deformation process, and has been used to solve practical technological problems.

5.1 *Design of Primary Deep-Drawing Blanks*

Using the FEM to design deep- drawing blanks, the influence of various factors in deep-drawing deformation can be correctly expressed. The basic idea of this method is: primary selection of blank shape- calculation of the distance S_i between the nodes on the outer-fringe and those on the inner-fringe of the flange area according to the results of the FEM analysis when the required punch depth is reached.

With regard to the inverse forming process, in primary selection of the blanks, take the nodes on the outer-fringe as starting points, substract S_i and obtain new outer-fringe curve, i.e. the reasonable shape and dimensions of the deep-drawing blanks (Fig. 5). Table 2 shows the comparison between the calculated results and the experimental data.

Using the present method to design blanks,

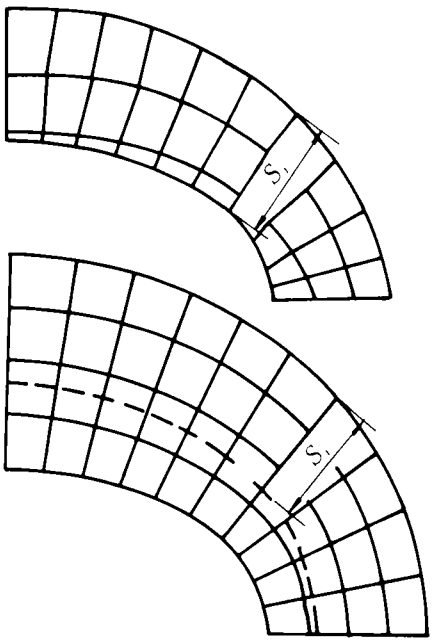

Fig. 5 Design method of blank shape and dimensions

Table 2 Comparison between calculated results and experimental data ($a/b = 1.6$)*

H	half major axis length A_0 /mm		half minor axis length B_0 /mm	
	cal.	exp.	cal.	exp.
10	37.8	36.2	28.1	29.2
15	10.7	39.1	32.1	32.9
20	13.6	12.0	35.6	36.0

* dimensions of the deep-drawing workpiece: $a = 30$ mm, $b = 18.75$ mm, earing height $\triangle H < 3$ mm

the computation time needed is less and the earing heights of the deep-drawing workpieces can be controlled under the required value.

5.2 *Formation Limit of Primary Deep-Drawing*

So-called formation limit of primary deep-drawing is referred to as the maximum deformation degree of plane blank deep-drawing, which can be reached under the condition that the material does not rupture, and generally it can be expressed by the maximum formation depth H_{max}. The condition ensuring that no rupture occurs is:

$$\sigma_{max} \leqslant \sigma_p \qquad (5)$$

where σ_{max} —the maximal tensile stress practically acted on the cups wall; σ_p —rupture stress of the cups wall.

The results of the FEM analysis are shown in Fig. 6, which indicates that the maximal formation depth H_{max} tends to decrease with increasing ratio a/b. This can be attributed to that when a remains constant, increasing a/b, i.e. decreasing b value will nake the curvature increase near the major axis on the inner-boundary of the deformation zone and cause the deformation to be more violent and the stress acted on the dangerous cross-section where the rupture occurs to be larger.

6 CONCLUSIONS

(1) The rigid-plastic finite element program developed in this paper can be used to analyse the deep-drawing deformation of the elliptic cups. The results obtained using this program are in good agreement with the experimental data. Therefore, this method is of high precision and the results are reliable.

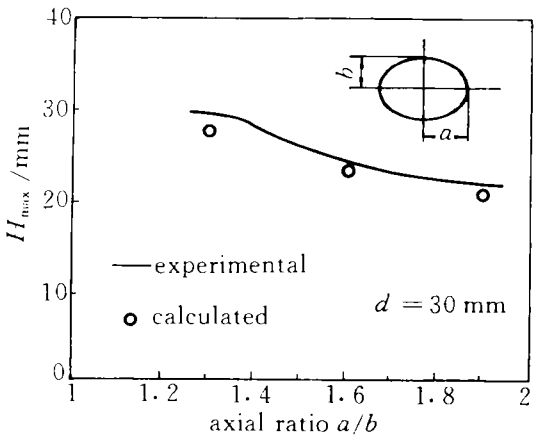

Fig. 6 Formation limit of deep-drawing

(2) The analysis by the FEM showed that in the deep-drawing processes of the elliptic cups, the particle moving velocity distribution, the stress and strain distributions and formation limit are all influenced by the axial ratio a/b.

(3)The present FEM program can be used to determine the reasonable blanks of the elliptic cups for primary deep-drawing and the formation limit, which is essential for laying out reasonable stamping processes.

REFERENCES

1 Li, Shuoben. Stamping Technology. Beijing: Mechanical Industry Press, 1982. 131—133.

2 Yang, Yuying *et al*. Electronic Technology, 1983, (9): 20—21.

3 Li, Naizhou; Liang, Bingwen. Forging and Stamping Technology, 1990, (2): 12—23.

4 Dou, Anping; Chu, Jiayou. Forging and Stamping Technology, 1991, (5): 25—27.

5 Li, Shunping; Li, Shuoben. Forging and Stamping Technology, 1991, (6): 15—20.

6 Kobayashi, S; Kim, J H *et al*. In: Proceedings of a Symposium on Mechanics of Sheet Metal Forming, California, October, 1997, 17—18.

7 Wang, Zhongren *et al*. Basic Mechanics of Plastic-Processing. Beijing: National Defence Industry Press, 1989. 101—112.